



# Effects of nutrient enrichment and skewed N:P ratios on physiology of scleractinian corals from Weizhou Island in the northern South China Sea

Zhiming Ning<sup>1</sup>, Kefu Yu<sup>1,2,\*</sup>, Yinghui Wang<sup>1</sup>, Fen Wei<sup>1</sup>, Zhiheng Liao<sup>1</sup>, Bin Yang<sup>3</sup>, Cao Fang<sup>1</sup>, Ronglin Xia<sup>1</sup>, Xueyong Huang<sup>1</sup>, Guodong Song<sup>4</sup>

<sup>1</sup>Guangxi Laboratory on the Study of Coral Reefs in the South China Sea, Coral Reef Research Centre of China, School of Marine Sciences, Guangxi University, Nanning 530004, PR China

<sup>2</sup>Southern Marine Science and Engineering Guangdong Laboratory, Zhuhai 519000, PR China

<sup>3</sup>Guangxi Key Laboratory of Marine Disaster in the Beibu Gulf, Beibu Gulf University, Qinzhou 535011, PR China

<sup>4</sup>Key Laboratory of Marine Chemistry Theory and Technology, Ministry of Education, Ocean University of China, Qingdao 266100, PR China

**ABSTRACT:** The availability of nitrogen (N) and phosphorus (P) is crucial for maintaining coral–dinoflagellate symbiosis, whereas excess nutrients and skewed N:P ratios are often associated with coral reef decline. It is thus essential to understand the general patterns of species-specific as well as dose-dependent responses of corals to elevated nutrient concentrations and skewed N:P ratios. Here, we found that the impacts of nutrient enrichment on the corals *Acropora millepora* and *Platygyra crosslandi* from Weizhou Island, South China Sea, were highly dependent on nutrient dose, N:P ratios, and coral species. Moderate nutrient enrichment (N: 19–140  $\mu\text{mol l}^{-1}$  and P: 0.5–1.5  $\mu\text{mol l}^{-1}$ ) did not lead to bleaching of either coral species, but their metabolic processes (calcification, nutrient uptake, and dinitrogen fixation) were affected. More depleted  $\delta^{13}\text{C}$  and lower dinitrogen fixation rates of *A. millepora* than of *P. crosslandi* indicated that *A. millepora* was more vulnerable to the disturbance of nutrient enrichment. However, N:P ratios ( $\pm$ SD) as high as  $106 \pm 10$  decreased the photosynthetic efficiency and nutrient uptake rates of *P. crosslandi*, indicating that this species may be vulnerable to high N:P ratios, although it was one of the dominant coral assemblages at Weizhou Island. The results provide an important basis for understanding coral reef degradation triggered by nutrients and a suggestion that coastal management should focus not only on the concentrations but also on the ratios of nutrients.

**KEY WORDS:** Coral · Nutrient enrichment · N:P ratio · Physiology · Metabolism rates

Resale or republication not permitted without written consent of the publisher

## 1. INTRODUCTION

Tropical scleractinian corals are holobionts consisting of the coral animal host, dinoflagellate algae, and a diverse assemblage of other microbes (Rohwer et al. 2002), the growth and stability of which are dependent on nutrient availability and metabolism (Morris et al. 2019). Because productivity of dinoflagellate algae is nitrogen (N)-limited in oligotrophic tropical waters, dinitrogen ( $\text{N}_2$ ) fixation by coral-

associated microbes is likely crucial for maintaining the coral–dinoflagellate symbiosis (Rädecker et al. 2015, Bednarz et al. 2017). Alternatively, dissolved organic N (DON) is also a dynamic pool of bioavailable N for sustaining coral metabolism (Crandall & Teece 2012). Conversely, phosphorus (P) is considered the ultimate limiting nutrient in coastal reefs (Ferrier-Pagès et al. 2016) that are subject to sewage or groundwater discharges (Tanaka et al. 2011, Ning et al. 2020).

\*Corresponding author: kefuyu@scsio.ac.cn

Coral bleaching is predominantly attributed to elevated temperature and light, but recent studies have unveiled nutritional mechanisms that can regulate bleaching (Wiedenmann et al. 2013, Morris et al. 2019). Nevertheless, studies on the functional significance of different coral species have focused on thermal tolerance rather than on the nutritional significance (Ezzat et al. 2017). Given the oligotrophic nature of reef-building corals, their symbiotic relationships may be particularly vulnerable to excess nutrients, which eventually lead to a significant loss of living corals (Yu 2012, Bell et al. 2014).

Nutrient enrichment generally increases the density and photosynthesis of symbiotic dinoflagellates, but decreases the rate of calcification (Fabricius 2005). The response of corals to nutrient enrichment is context dependent, varying with coral taxa and morphology, enrichment source, and nutrient dose level (Koop et al. 2001, Shantz & Burkepile 2014, Blanckaert et al. 2020). For example, moderate nutrient enrichment has no effect on the calcification of *Porites cylindrica*, whereas the calcification of *Montipora digitata* declines under nutrient enrichment (Tanaka et al. 2017). Therefore, more extensive experiments should be conducted to understand the general patterns of coral species-specific responses to a wide range of nutrient doses.

The effects of nutrient enrichment on coral holobionts are not necessarily caused by the concentration of nutrients, but by the P starvation of the algal symbionts caused by high N:P ratios (Rosset et al. 2017). For instance, the carbon fixation rate and the translocation of photosynthates to the animal host decreased when only nitrate was experimentally added to the seawater (Ezzat et al. 2015). This is because P starvation can change the composition of lipids in the thylakoid membrane structure and then increase the susceptibility of corals to temperature- and light-induced bleaching (Wiedenmann et al. 2013). However, the effects of N:P ratios on coral holobionts have been investigated only in a few coral species from limited geographic locations in the world, and coral species-specific responses to high N:P ratios are not yet clear.

Weizhou Island (21° 00'–21° 10' N, 109° 00'–109° 15' E), located in a relatively high-latitude area in the northern South China Sea (Fig. 1), is a potential refuge from climate change for corals that are often threatened by eutrophication attributed to anthro-

pogenic activities (Yu et al. 2019). Thus, to test the hypothesis that the responses of corals around the island to elevated nutrient concentrations and skewed ratios are species-specific as well as dose-dependent, we collected branching coral *Acropora millepora* and massive coral *Platygyra crosslandi* and quantified their  $\delta^{13}\text{C}$ ,  $\delta^{15}\text{N}$ , algal biomass, and metabolic rates, including photosynthetic yield of dinoflagellates, calcification, nutrient fluxes, and diazotroph-derived N (DDN) assimilation rates. With these comprehensive data, we were able to assess (1) the extent of coral responses to eutrophication, (2) the species-specific responses of corals to a skewed N:P ratio, and (3) whether corals at Weizhou Island are affected by eutrophication.

## 2. MATERIALS AND METHODS

### 2.1. Study site

Weizhou Island is a volcanic island located in the Beibu Gulf, northern South China Sea (Fig. 1), and its relatively high subtropical latitude provides an ideal habitat for coral growth. However, the mean living coral cover around Weizhou Island has decreased from ~42 % in 1984 to ~10 % in 2015, and the massive coral *Platygyra crosslandi* is one of the dominant species, while cover of the branching coral *Acropora millepora* is <1 % (Yu et al. 2019). The rapid coral reef degeneration is attributed to escalating anthropogenic impacts such as those of domestic and aquaculture wastewater discharges (Yu et al. 2019). The concentrations of dissolved inorganic nitrogen and phosphorus (DIN and DIP) at Weizhou Island during 2018–2019 were 2.31–11.47 and 0.02–0.43  $\mu\text{mol l}^{-1}$ , respectively, and the N:P ratio ranged from 12 to 350 (Ning et al. 2020). The increasing anthropogenic pol-

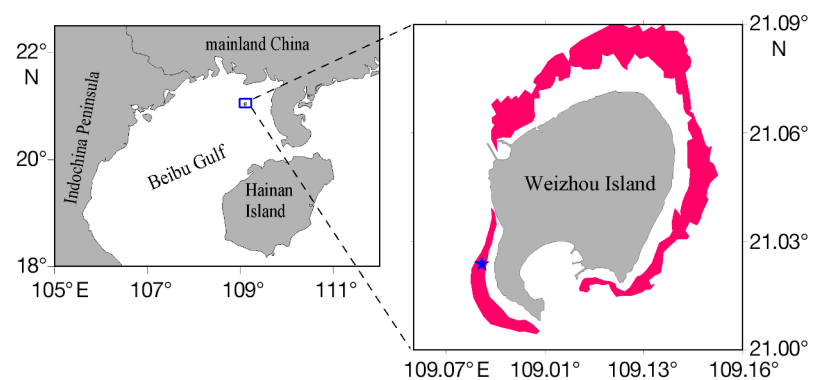


Fig. 1. Study location and sampling station (blue star). The red areas represent areas covered by living coral

lution in recent years has resulted in an increasing trend in DIN concentration, whereas the DIP concentration has changed little over the same period; thus, the N:P ratio has gradually increased (Yu et al. 2019).

## 2.2. Coral preparation and acclimatization

We collected 4 *A. millepora* colonies and 3 *P. crosslandi* colonies from the sampling station (Fig. 1) in April 2018. The colonies of both species were cut into 20 fragments (about 100 cm<sup>2</sup>) and were then transferred into 5 flow-through aquariums (4 *A. millepora* fragments and 4 *P. crosslandi* fragments in each aquarium) where fresh seawater was continuously supplied and allowed to acclimate under natural sunlight (irradiance was ~400  $\mu\text{mol photons m}^{-2} \text{s}^{-1}$  in the morning and ~520  $\mu\text{mol photons m}^{-2} \text{s}^{-1}$  in the afternoon). The nutrient concentrations in the respective seawater flowing into 4 out of 5 aquariums were amended to gradient concentrations (Table 1) by adding different doses of NH<sub>4</sub>Cl, NaNO<sub>3</sub>, and KH<sub>2</sub>PO<sub>4</sub> stock solution (100 mmol l<sup>-1</sup>), and the remaining aquarium without nutrients added was regarded as the 'control' treatment. The nutrient concentrations in nutrient-enriched groups I–IV were as high as those used in earlier eutrophication experiments on reefs (Lam et al. 2015, Reich et al. 2020).

## 2.3. Flow-through reactor (FTR) incubation

The FTR consisted of a 2 l Plexiglas column (10 cm internal diameter) and 2 lids designed by Rao et al. (2007), in which radial grooves were milled around the inflow and outflow ports. The reactor was equipped with a Teflon-coated magnetic stir bar to ensure that the seawater it contained was evenly mixed. Plexiglas columns were connected to inflow and outflow containers with 0.3 cm ID Teflon tubing.

After 1 wk of acclimation, coral fragments from different aquariums were each transferred into separate

FTRs (i.e. only 1 fragment in each FTR), and seawater was pumped into the corresponding FTR from the bottom up at a flow rate of 20 ml min<sup>-1</sup>. Similarly, different doses of NH<sub>4</sub>Cl, NaNO<sub>3</sub>, and KH<sub>2</sub>PO<sub>4</sub> stock solution were added into the influent seawater to obtain gradients of nutrient concentrations (Table 1). Thus, there were 4 *A. millepora* fragments and 4 *P. crosslandi* fragments as replicate samples in each group.

Measurement of each FTR was conducted once during daytime. The temperature, pH, dissolved oxygen (DO), and total alkalinity (TA) of the influent and effluent seawater were measured. At the same time, water samples were collected and filtered with 0.45  $\mu\text{m}$  pore-size syringe filters and were frozen at -20°C until later nutrient analysis. The effective photosynthetic efficiency ( $\Phi_{\text{PSII}}$ ) of all coral fragments was measured between 09:00 and 11:00 h to ensure that the light conditions (irradiance of ~400  $\mu\text{mol photons m}^{-2} \text{s}^{-1}$ ) were relatively constant. A photosynthesis yield analyzer (mini-PAM, Walz) applied 3  $\mu\text{s}$  pulses of weak light (<0.15  $\mu\text{mol photons m}^{-2} \text{s}^{-1}$ ) and saturation pulses of white light (4500  $\mu\text{mol photons m}^{-2} \text{s}^{-1}$ ) to detect the minimum ( $F$ ) and maximum ( $F_m'$ ) fluorescence of light-adapted samples, respectively, and thus  $\Phi_{\text{PSII}} = (F_m' - F) / F_m'$  (Xu et al. 2017). Measurement of each FTR could be completed within 10 min.

## 2.4. <sup>15</sup>N<sub>2</sub> added incubation for N<sub>2</sub> fixation measurement

After the coral incubation, seawater in FTRs for the <sup>15</sup>N<sub>2</sub> incubation experiment was filtered (0.2  $\mu\text{m}$ ), and then 10% volume of the incubation columns was replaced by <sup>15</sup>N<sub>2</sub>-enriched seawater (details in the following paragraph). The valves on the inflow and outflow tubes of each column were closed so that every column was closed. A magnetic stirrer was used to mix the seawater inside the column. In parallel, duplicate corals were also incubated in seawater without <sup>15</sup>N<sub>2</sub>-enriched seawater added.

Table 1. Nutrient concentrations ( $\mu\text{mol l}^{-1}$ ) and N:P ratios (mean  $\pm$  SD) in influent seawater during incubations. DON: dissolved organic nitrogen; DIP: dissolved inorganic phosphorus; DOP: dissolved organic phosphorus

Group	NH <sub>4</sub> <sup>+</sup>	NO <sub>3</sub> <sup>-</sup>	DON	DIP	DOP	N:P
Control	1.56 $\pm$ 0.06	2.21 $\pm$ 0.11	19.82 $\pm$ 1.03	0.23 $\pm$ 0.02	2.97 $\pm$ 0.04	16.4 $\pm$ 2.1
I	34.46 $\pm$ 2.17	18.96 $\pm$ 1.19	19.16 $\pm$ 1.93	0.54 $\pm$ 0.04	3.49 $\pm$ 0.32	106.5 $\pm$ 9.6
II	32.49 $\pm$ 2.39	102.91 $\pm$ 2.22	30.78 $\pm$ 10.11	1.50 $\pm$ 0.11	4.29 $\pm$ 0.19	93.3 $\pm$ 7.1
III	32.23 $\pm$ 1.31	191.65 $\pm$ 4.06	22.52 $\pm$ 3.18	3.92 $\pm$ 0.15	4.23 $\pm$ 0.53	58.2 $\pm$ 2.2
IV	30.20 $\pm$ 1.16	317.71 $\pm$ 3.65	21.78 $\pm$ 2.68	8.13 $\pm$ 0.15	4.03 $\pm$ 0.29	43.3 $\pm$ 1.1

$^{15}\text{N}_2$ -enriched seawater was prepared as described by Großkopf et al. (2012). Filtered (0.2  $\mu\text{m}$ ) seawater was degassed for 1 h using a vacuum pump and was then transferred into a 2 l Tedlar bag without a headspace. After 20 ml  $^{15}\text{N}_2$  (98 atom%  $^{15}\text{N}_2$ ) were injected into the bag, it was horizontally shaken for 12 h to complete dissolution of the added  $^{15}\text{N}_2$  gas. To obtain the atom%  $^{15}\text{N}$  in the dissolved  $\text{N}_2$  pool, an aliquot of  $^{15}\text{N}_2$ -enriched seawater was sampled from the bag and transferred to a 12 ml Exetainer vial (Labco); the  $\delta^{15}\text{N}$  of the dissolved  $\text{N}_2$  pool was then measured by membrane inlet mass spectrometry (MIMS).

After 24 h of incubation, coral fragments were collected from the incubation columns, rinsed with filtered seawater, and frozen at  $-20^\circ\text{C}$  for later analysis of the coral tissue and dinoflagellate fractions.

### 2.5. Sample analysis

The coral tissue was completely removed from the skeleton using a Waterpik containing filtered seawater and was then homogenized with a Potter tissue grinder. The homogenate was centrifuged at  $2000 \times g$  (10 min at  $4^\circ\text{C}$ ) to pellet the zooxanthellae, and the supernatant was transferred into 50 ml polypropylene tubes. Respective tubes containing tissues or zooxanthellae were frozen in liquid nitrogen and freeze-dried. The biomass of dinoflagellates and tissue content were then quantified via their dry weights and normalized to the coral surface area (Grover et al. 2002). Skeletal surface area was measured using the aluminum foil method (Marsh 1970, Xu et al. 2017).

The  $^{13}\text{C}$  and  $^{15}\text{N}$  in coral tissue and symbiotic dinoflagellates were quantified with a mass spectrometer (Mat 253; Thermo Fisher Scientific) coupled via a C/N/S elemental analyzer (Flash EA; Thermo Fisher Scientific). The precision for  $^{13}\text{C}$  and  $^{15}\text{N}$  was  $<0.2\%$ .

Total alkalinity (TA) was estimated by Gran titration using pre-standardized HCl and was corrected against Dickson reference material (Batch 122) (McMahon et al. 2013). Calibration of the pH probe was done using standards (buffers of pH 4, 7, and 10). The measurement precisions for pH and TA were both  $<0.2\%$ . Dissolved inorganic carbon (DIC) concentrations and saturation of aragonite ( $\Omega_{\text{Ar}}$ ) were calculated from salinity, temperature, TA, and pH using the Excel macro CO2SYS (Lewis & Wallace 1998). Nutrient concentrations were determined using an autoanalyzer (QuAAtro, SEAL Analytical).

The measurement precisions for the  $\text{NO}_3^-$ ,  $\text{NO}_2^-$ ,  $\text{NH}_4^+$ , DIP, total dissolved nitrogen (TDN), and total dissolved phosphorus (TDP) analyses were  $<6\%$  CV (Ning et al. 2019). DON concentration was obtained from the difference between TDN concentration and DIN ( $= \text{NO}_3^- + \text{NO}_2^- + \text{NH}_4^+$ ) concentration, and dissolved organic P (DOP) concentration was obtained from the difference between TDP concentration and DIP concentration.

### 2.6. Calculations and statistical analyses

Uptake rates ( $\mu\text{mol cm}^{-2} \text{h}^{-1}$ ) of DIC, TA, and nutrients from coral holobionts were calculated from the differences in concentrations of DIC, TA, and nutrients between influent and effluent seawater; flow rates; and the coral surface area, according to Eq. (1) (Ning et al. 2020). The negative values of the rates represented release rates from the coral to the seawater:

$$F = (C_{\text{in}} - C_{\text{out}}) \times R / S \quad (1)$$

where  $C_{\text{in}}$  and  $C_{\text{out}}$  are the concentrations of DIC, TA, and nutrients in the influent and effluent seawater, respectively.  $R$  is the flow rate, and  $S$  is the surface area of corals.

Calcification rate of coral holobionts can be calculated by TA release rate/ $-2$ , as 2 moles of TA are produced/consumed for every 1 mole of  $\text{CaCO}_3$  dissolved/precipitated, and the negative value of the rate represents the  $\text{CaCO}_3$  dissolution rate.

DDN assimilation rates by coral tissues and dinoflagellates were calculated based on the final isotopic composition of the particulate N (PN) after the incubation using the following equation according to Eq. (2) from Mohr et al. (2010):

$$\text{DDN assimilation} = \frac{(A_{\text{sample}}^{\text{PN}} - A_{\text{control}}^{\text{PN}})}{(A_{\text{N}_2} - A_{\text{control}}^{\text{PN}})} \times \frac{[\text{PN}]}{t} \quad (2)$$

where  $A$  = atom%  $^{15}\text{N}$  in the PN in incubations to which  $^{15}\text{N}_2$ -enriched seawater was added ( $A_{\text{sample}}^{\text{PN}}$ ), in incubations ( $A_{\text{control}}^{\text{PN}}$ ) without  $^{15}\text{N}_2$ -enriched seawater added, or in the dissolved  $\text{N}_2$  pool ( $A_{\text{N}_2}$ ).  $A_{\text{N}_2}$  was calculated from the  $\delta^{15}\text{N}$  measured by MIMS;  $t$  is the incubation time; and  $[\text{PN}]$  is the PN content of the sample at the end of the incubation normalized per  $\text{cm}^2$  of coral skeletal surface area.

All results are expressed as mean  $\pm$  standard deviation (SD). Assumptions of normality and homogeneity of variances were tested using Shapiro–Wilk and Levene's tests, respectively. When the data did not meet the assumptions, they were logarithmically

transformed prior to subsequent ANOVAs (referring to biomass of symbiotic dinoflagellates in this case). A 2-way ANOVA was then used to test for significant differences of physiological parameters between corals (*A. millepora* and *P. crosslandi*) and nutrients (5 levels). The effect of nutrients on physiological parameters for each species was tested using a 1-way ANOVA, and the Tukey test was used for post hoc multiple comparisons for further analysis of significance. Pearson's correlation analysis with a 2-tailed test of significance was used to evaluate the relationships between the measured parameters. All statistical analyses were carried out with SPSS (version 22.0), and statistical significance was judged using the criterion  $p < 0.05$ .

### 3. RESULTS

After FTR incubation of branching coral *Acropora millepora* and massive coral *Platygyra crosslandi* under different nutrient conditions, we found that the biomass and  $\Phi_{\text{PSII}}$  of symbiotic dinoflagellates,  $\delta^{15}\text{N}$ , and  $\delta^{13}\text{C}$  were statistically significantly different between the 2 coral species, and all of these parameters and metabolic (calcification, nutrient fluxes, and DDN) rates varied significantly under different nutrient conditions; the interactive effect (coral  $\times$  nutrient) was significant for almost all physiological parameters with the exception of calcification and fluxes of DIC,  $\text{NO}_3^-$ , and DIP (Table 2).

#### 3.1. Symbiotic biomass, $\Phi_{\text{PSII}}$ , and calcification rates of 2 coral species under different nutrient conditions

Biomass of symbiotic dinoflagellates in *P. crosslandi* ( $4.74 \pm 1.55 \text{ mg cm}^{-2}$ ) was 2–6 times the level in *A. millepora* ( $1.41 \pm 0.40 \text{ mg cm}^{-2}$ ); the algal biomass of corals from Weizhou Island was affected by nutrient enrichment (2-way ANOVA,  $F_{4,30} = 9.25$ ,  $p < 0.001$ ). Specifically, the algal biomass of *P. crosslandi* was 2.5 times lower in group IV ( $2.39 \pm 0.59 \text{ mg cm}^{-2}$ ) than in other groups (Fig. 2a). The  $\Phi_{\text{PSII}}$  of symbiotic dinoflagellates differed significantly between *A. millepora* ( $0.69 \pm 0.02$ ) and *P. crosslandi* ( $0.62 \pm 0.09$ ) (2-way ANOVA,  $F_{1,30} = 112$ ,  $p < 0.001$ ) and also differed significantly under varied nutrient conditions (2-way ANOVA,  $F_{4,30} = 44.2$ ,  $p < 0.001$ ); in particular, the value of *P. crosslandi* in group I was as low as  $0.47 \pm 0.06$  (Fig. 2b).

There was no significant difference in calcification rate between the 2 coral species (2-way ANOVA,  $F_{1,30} = 1.64$ ,  $p = 0.211$ ), but calcification rates were statistically significantly different between different nutrient conditions (2-way ANOVA,  $F_{4,30} = 221$ ,  $p < 0.001$ ). The calcification rate decreased from  $0.014 \pm 0.007 \mu\text{mol cm}^{-2} \text{ h}^{-1}$  in the control group to  $0.010 \pm 0.016 \mu\text{mol cm}^{-2} \text{ h}^{-1}$  in groups I and II with moderate nutrient concentrations (DIN: 19–140  $\mu\text{mol l}^{-1}$  and DIP: 0.5–1.5  $\mu\text{mol l}^{-1}$ ), whereas  $\text{CaCO}_3$  was turned to net dissolution in groups III and IV when the concentrations of DIN and DIP in seawater were  $>225$  and  $>3.9 \mu\text{mol l}^{-1}$ , respectively (Fig. 2c). In particular, the

Table 2. Results of ANOVA for physiological parameters between corals (*Acropora millepora* and *Platygyra crosslandi*) and nutrients (5 levels; see Table 1). Significant results ( $p < 0.05$ ) are indicated in **bold**. DIC: dissolved inorganic carbon; DON: dissolved organic nitrogen; DIP: dissolved inorganic phosphorus; DOP: dissolved organic phosphorus; DDN: diazotroph-derived nitrogen

Parameter	Coral species			Nutrient conditions			Coral $\times$ nutrient		
	df	<i>F</i>	<i>p</i>	df	<i>F</i>	<i>p</i>	df	<i>F</i>	<i>p</i>
Biomass of dinoflagellates	<b>1</b>	<b>270</b>	<b>&lt;0.001</b>	4	<b>9.25</b>	<b>&lt;0.001</b>	4	<b>12.8</b>	<b>&lt;0.001</b>
$\Phi_{\text{PSII}}$ of dinoflagellates	<b>1</b>	<b>112</b>	<b>&lt;0.001</b>	4	<b>44.2</b>	<b>&lt;0.001</b>	4	<b>52.5</b>	<b>&lt;0.001</b>
$\delta^{15}\text{N}$ of dinoflagellates	<b>1</b>	<b>32.0</b>	<b>&lt;0.001</b>	4	<b>30.6</b>	<b>&lt;0.001</b>	4	<b>22.2</b>	<b>&lt;0.001</b>
$\delta^{13}\text{C}$ of dinoflagellates	<b>1</b>	<b>31.6</b>	<b>&lt;0.001</b>	4	<b>3.65</b>	<b>0.015</b>	4	<b>11.4</b>	<b>&lt;0.001</b>
$\delta^{15}\text{N}$ of coral tissue	<b>1</b>	<b>744</b>	<b>&lt;0.001</b>	4	<b>137</b>	<b>&lt;0.001</b>	4	<b>63.3</b>	<b>&lt;0.001</b>
$\delta^{13}\text{C}$ of coral tissue	<b>1</b>	<b>409</b>	<b>&lt;0.001</b>	4	<b>2.82</b>	<b>0.043</b>	4	<b>5.67</b>	<b>0.002</b>
Calcification rates	1	1.64	0.211	4	<b>221</b>	<b>&lt;0.001</b>	4	0.867	0.495
DIC flux	1	2.32	0.139	4	<b>86.8</b>	<b>&lt;0.001</b>	4	1.40	0.259
$\text{NH}_4^+$ flux	<b>1</b>	<b>54.4</b>	<b>&lt;0.001</b>	4	<b>77.6</b>	<b>&lt;0.001</b>	4	<b>24.1</b>	<b>&lt;0.001</b>
$\text{NO}_3^-$ flux	1	0.798	0.379	4	<b>163</b>	<b>&lt;0.001</b>	4	1.58	0.206
DON flux	1	0.118	0.733	4	<b>114</b>	<b>&lt;0.001</b>	4	<b>7.98</b>	<b>&lt;0.001</b>
DIP flux	1	1.57	0.220	4	<b>100</b>	<b>&lt;0.001</b>	4	0.817	0.525
DOP flux	1	0.911	0.348	4	<b>512</b>	<b>&lt;0.001</b>	4	<b>23.8</b>	<b>&lt;0.001</b>
DDN by dinoflagellates	<b>1</b>	<b>2814</b>	<b>&lt;0.001</b>	4	<b>2729</b>	<b>&lt;0.001</b>	4	<b>1924</b>	<b>&lt;0.001</b>
DDN by coral tissue	<b>1</b>	<b>253</b>	<b>&lt;0.001</b>	4	<b>4160</b>	<b>&lt;0.001</b>	4	<b>626</b>	<b>&lt;0.001</b>

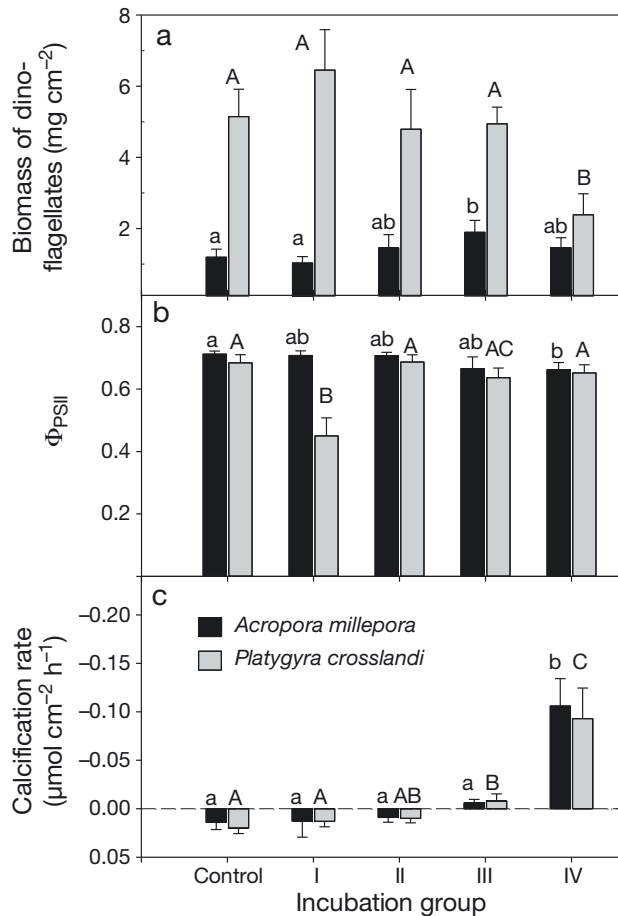


Fig. 2. (a) Biomass and (b) effective photosynthetic efficiency ( $\Phi_{PSII}$ ) of symbiotic dinoflagellates, and (c) calcification rates of corals *Acropora millepora* and *Platygyra crosslandi* incubated in 5 different nutrient conditions (see Table 1). Negative values of calcification rates represent  $\text{CaCO}_3$  dissolution rates. The error bars show SD, and different letters above histograms denote statistical differences among varied nutrient conditions (Tukey tests,  $p < 0.05$ )

calcification rate in group IV with the highest nutrient concentrations ( $0.099 \pm 0.022 \mu\text{mol cm}^{-2} \text{h}^{-1}$ ) was significantly different from that of other groups (Tukey,  $p < 0.001$ , Fig. 2c).

### 3.2. $\delta^{13}\text{C}$ and $\delta^{15}\text{N}$ of 2 coral holobionts under different nutrient conditions

The  $\delta^{13}\text{C}$  in coral tissue of *A. millepora* ( $-17.85 \pm 0.37\text{‰}$ ) was depleted by 10% in comparison with that of *P. crosslandi* ( $-16.09 \pm 0.32\text{‰}$ ) (Fig. 3a). Tissue  $\delta^{13}\text{C}$  differed significantly under different nutrient conditions (2-way ANOVA,  $F_{4,30} = 2.82$ ,  $p = 0.043$ ). The  $\delta^{13}\text{C}$  in tissue of *P. crosslandi* was slightly depleted with increasing nutrient concentrations and

was most depleted in group IV ( $-16.49 \pm 0.19\text{‰}$ ), whereas the most depleted  $\delta^{13}\text{C}$  in tissue of *A. millepora* was observed in group I ( $-18.36 \pm 0.32\text{‰}$ ) (Fig. 3a).

The  $\delta^{13}\text{C}$  in symbiotic dinoflagellates of *A. millepora* ( $-16.68 \pm 0.51\text{‰}$ ) was depleted by 3% in comparison with that of *P. crosslandi* ( $-16.17 \pm 0.37\text{‰}$ ) (2-way ANOVA,  $F_{1,30} = 31.6$ ,  $p < 0.001$ ). Similar to the variation in tissue  $\delta^{13}\text{C}$ , algal  $\delta^{13}\text{C}$  was significantly varied with different nutrient conditions (2-way ANOVA,  $F_{4,30} = 3.65$ ,  $p = 0.015$ ). The most depleted  $\delta^{13}\text{C}$  in dinoflagellates of *A. millepora* was observed in group I ( $-17.35 \pm 0.27\text{‰}$ ), while that of *P. crosslandi* was observed in group IV ( $-16.65 \pm 0.21\text{‰}$ ) (Fig. 3b). In addition,  $\delta^{13}\text{C}$  in dinoflagellates was positively correlated to  $\delta^{13}\text{C}$  in tissue (Pearson,  $r = 0.684$ ,  $p < 0.001$ ) and to biomass of dinoflagellates (Pearson,  $r = 0.566$ ,  $p < 0.001$ , Table 3).

The  $\delta^{15}\text{N}$  decreased from coral tissue ( $7.73 \pm 1.76\text{‰}$ ) to dinoflagellates ( $5.69\text{‰} \pm 0.46\text{‰}$ ), and both showed a significant effect between nutrients (2-way ANOVA,  $F_{4,30} = 30.6$  for dinoflagellates and  $F_{4,30} = 137$  for tissue,  $p < 0.001$ ) and coral species (2-way ANOVA,  $F_{1,30} = 32.0$  for dinoflagellates and  $F_{1,30} = 744$  for tissue,  $p < 0.001$ ). In groups II, III, and IV with high nutrient concentrations,  $\delta^{15}\text{N}$  in tissue of *A. millepora* and *P. crosslandi* was enriched by 50 and 16%, respectively (Fig. 3c). Conversely,  $\delta^{15}\text{N}$  in dinoflagellates of both species was depleted by 13% under high nutrient concentrations (Fig. 3d). In addition,  $\delta^{15}\text{N}$  in tissue was negatively correlated with  $\delta^{13}\text{C}$  in tissue (Pearson,  $r = -0.618$ ,  $p < 0.001$ , Table 3).

### 3.3. Nutrient fluxes between the corals and seawater under different nutrient conditions

Both *A. millepora* and *P. crosslandi* assimilated  $\text{NH}_4^+$  and  $\text{NO}_3^-$ , at rates of 0.03–0.22 and 0.02–0.46  $\mu\text{mol cm}^{-2} \text{h}^{-1}$ , respectively, and released DON at rates of 0.09–1.22  $\mu\text{mol cm}^{-2} \text{h}^{-1}$  (Fig. 4a–c). The uptake rates of nutrients were higher in the nutrient-enriched groups than in the control group. In particular,  $\text{NO}_3^-$  uptake rate by *P. crosslandi* was 50 times higher under nutrient enrichment than in the control group, but  $\text{NO}_3^-$  was released from the coral to the seawater in group IV at a rate of  $0.29 \pm 0.21 \mu\text{mol cm}^{-2} \text{h}^{-1}$  (Fig. 4b). Similarly, the DON flux in group IV differed significantly from other groups (Tukey,  $p < 0.001$ , Fig. 4c).

In the control group, coral holobionts assimilated DIP at rate of  $0.001 \pm 0.001 \mu\text{mol cm}^{-2} \text{h}^{-1}$  and released DOP at rate of  $0.002 \pm 0.002 \mu\text{mol cm}^{-2} \text{h}^{-1}$ ;

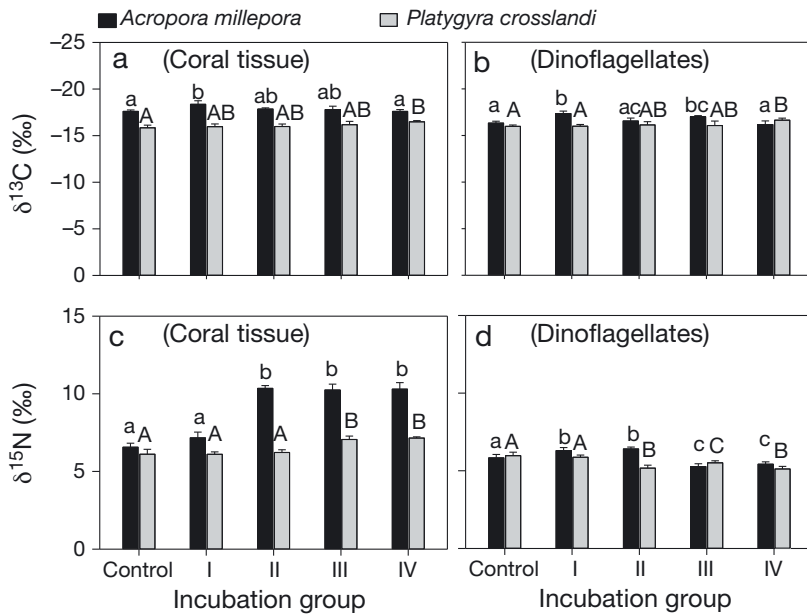


Fig. 3. (a,b)  $\delta^{13}\text{C}$  and (c,d)  $\delta^{15}\text{N}$  in coral tissue and dinoflagellates of corals *Acropora millepora* and *Platygyra crosslandi* incubated in 5 different nutrient conditions (see Table 1). The error bars show SD, and different letters above histograms denote statistical differences among varied nutrient conditions (Tukey tests,  $p < 0.05$ )

under nutrient enrichment, both DIP and DOP were assimilated by coral holobionts at rates of  $0.006 \pm 0.006$  and  $0.039 \pm 0.030 \mu\text{mol cm}^{-2} \text{h}^{-1}$ , respectively, with the exception in group IV in which both DIP and DOP were released from the coral into the seawater at rate of  $-0.015 \pm 0.013 \mu\text{mol cm}^{-2} \text{h}^{-1}$  and  $-0.058 \pm 0.021 \mu\text{mol cm}^{-2} \text{h}^{-1}$ , respectively (Tukey,  $p < 0.001$ , Fig. 4d,e). In particular, the highest DOP uptake rate ( $0.070 \pm 0.011 \mu\text{mol cm}^{-2} \text{h}^{-1}$ ) was observed in group I, in which the DIN:DIP ratio in seawater was the highest (Fig. 4e).

DIC was released from coral holobionts into seawater in all incubation groups and significantly increased from  $0.12 \pm 0.14 \mu\text{mol cm}^{-2} \text{h}^{-1}$  in group I and the control group to  $0.71 \pm 0.21 \mu\text{mol cm}^{-2} \text{h}^{-1}$  in groups II and III, and then to  $1.48 \pm 0.23 \mu\text{mol cm}^{-2} \text{h}^{-1}$  in group IV (Fig. 4f). Furthermore, correlation analysis showed that the calcification rate was positively related to the DIC flux (Pearson,  $r = 0.854$ ,  $p < 0.001$ , Table 3).

### 3.4. DDN assimilation rates by 2 coral species under different nutrient conditions

Under natural conditions (i.e. the control group), more than 99% of the DDN was assimilated by coral tissue rather than symbiotic dinoflagellates, but the

DDN assimilation by dinoflagellates increased with increasing nutrient concentrations (2-way ANOVA,  $F_{4,30} = 2729$ ,  $p < 0.001$ , Fig. 5). The DDN assimilation by tissue of *P. crosslandi* was greater than that of *A. millepora* (2-way ANOVA,  $F_{1,30} = 253$ ,  $p < 0.001$ , Table 2). In tissue of *A. millepora*, the DDN assimilation rate decreased from  $39.06 \pm 5.56 \mu\text{mol cm}^{-2} \text{h}^{-1}$  in control group to  $13.62 \pm 3.20 \mu\text{mol cm}^{-2} \text{h}^{-1}$  in group II, and then to  $0.96 \pm 0.47 \mu\text{mol cm}^{-2} \text{h}^{-1}$  in groups II, III, and IV; in tissue of *P. crosslandi*, DDN assimilation rate in groups I and IV was 65% lower than that in other groups ( $95.75 \pm 7.61 \mu\text{mol cm}^{-2} \text{h}^{-1}$ ) (Fig. 5a). In dinoflagellates of both species, the DDN assimilation rate in groups III and IV was significantly higher than in other groups (Tukey,  $p < 0.001$ , Fig. 5b). Furthermore, DDN assimilation by tissue was negatively related to the  $\delta^{15}\text{N}$  in tissue (Pearson,  $r = -0.732$ ,  $p < 0.001$ ), and DDN assimilation by dinoflagellates was also negatively related to the  $\delta^{15}\text{N}$  in dinoflagellates (Pearson,  $r = -0.475$ ,  $p = 0.002$ ).

## 4. DISCUSSION

The effects of nutrients on the physiology of corals were caused not only by the concentrations but also by the skewed N:P ratios, and we found that different species of corals have different responses to nutrient enrichment. Based on the data of biomass and  $\Phi_{\text{PSII}}$  of symbiotic dinoflagellates and  $\delta^{15}\text{N}$ ,  $\delta^{13}\text{C}$ , and metabolic (calcification, nutrient fluxes, and DDN) rates of coral holobionts, we first assess the extent of coral responses to different nutrient concentrations, then discuss the effects of N:P ratios on different physiological parameters of corals, and finally compare the differences in the responses of the 2 corals to nutrient enrichments.

### 4.1. Effects of nutrient enrichment on physiology of coral holobionts

The algal biomass of corals from Weizhou Island was affected by nutrient enrichment despite the absence of coral bleaching. Specifically, low algal biomass was observed in experimental group IV that

Table 3. Pearson's correlation statistics between the measured parameters. Significant results ( $p < 0.05$ ) are indicated in **bold**. Abbreviations as in Table 2

Parameter	Dinoflagellate biomass	$\Phi_{PSII}$	Dinoflagellate $\delta^{15}N$	Dinoflagellate $\delta^{13}C$	Tissue $\delta^{15}N$	Tissue $\delta^{13}C$	Calcification	DIC flux	$NH_4^+$ flux	$NO_3^-$ flux	DON flux	DIP flux	DOP flux	DDN by tissue
$\Phi_{PSII}$	<b>-0.61</b>													
Dinoflagellates $\delta^{15}N$	-0.16	0.08												
Dinoflagellates $\delta^{13}C$	<b>0.57</b>	-0.30	-0.07											
Tissue $\delta^{15}N$	<b>-0.57</b>	0.26	0.00	-0.30										
Tissue $\delta^{13}C$	<b>0.86</b>	-0.45	-0.32	<b>0.68</b>	<b>-0.62</b>									
Calcification	0.30	0.00	<b>0.51</b>	0.00	-0.39	0.09								
DIC flux	0.22	-0.10	<b>0.52</b>	-0.06	-0.42	-0.02	<b>0.85</b>							
$NH_4^+$ flux	-0.05	-0.10	<b>0.53</b>	-0.31	-0.03	-0.38	0.39	<b>0.52</b>						
$NO_3^-$ flux	0.25	0.05	0.10	-0.11	-0.01	0.04	<b>0.66</b>	0.43	0.23					
DON flux	0.33	-0.01	0.45	0.14	-0.27	0.11	<b>0.90</b>	<b>0.78</b>	0.29	<b>0.57</b>				
DIP flux	0.29	-0.07	0.26	-0.05	-0.20	0.06	<b>0.79</b>	<b>0.64</b>	0.39	<b>0.89</b>	<b>0.68</b>			
DOP flux	0.29	-0.28	0.45	-0.16	-0.25	-0.06	<b>0.73</b>	<b>0.67</b>	<b>0.75</b>	<b>0.67</b>	<b>0.60</b>	<b>0.81</b>		
DDN by tissue	<b>0.71</b>	-0.05	-0.19	<b>0.54</b>	<b>-0.73</b>	<b>0.78</b>	0.36	0.20	-0.17	0.30	0.36	0.33	0.15	
DDN by dinoflagellates	-0.01	-0.04	<b>-0.48</b>	0.04	0.30	0.06	<b>-0.54</b>	<b>-0.53</b>	-0.16	0.14	<b>-0.56</b>	-0.01	-0.14	0.01

was exposed to the highest nutrient enrichment. On the other hand, nutrient enrichment also led to a decrease in calcification, because the addition of nutrients can enhance organic metabolism (respiration and photosynthesis), which plays a role in determining the DIC in the overlying water column (Glud et al. 2008, Lantz et al. 2017), and elevated DIC exacerbates the decrease in coral calcification (Meyer et al. 2016).

In this study, coral  $\delta^{13}C$  was slightly depleted with increasing nutrient concentrations, indicating an increasing degree of heterotrophy by the coral host (Risk et al. 1994, Heikoop et al. 2000, Xu et al. 2021). Meanwhile, tissue  $\delta^{15}N$  was enriched under nutrient enrichments. This may be because corals that are more heterotrophic harbor smaller communities of  $N_2$  fixers than corals that are more autotrophic (Pogoreutz et al. 2017b), and less uptake of light  $^{14}N_2$  by  $N_2$  fixers may ultimately result in enriched  $\delta^{15}N$  values (Lesser et al. 2007). Thus, the  $\delta^{15}N$  values in tissue were negatively related to DDN assimilation by tissue and  $\delta^{13}C$  values.

Algal symbionts may translocate fewer products to the host cells when coral is bleaching (Hillyer et al. 2018), whereas DDN may constitute an additional N source for bleaching corals (Pogoreutz et al. 2017a, Bednarz et al. 2019). In this study, nutrient-stimulated coral heterotrophy led to increased DDN assimilation by symbiotic dinoflagellates but to decreased DDN assimilation by tissue. This is consistent with the previous finding that sugar-induced bleaching/stimulated  $N_2$  fixation led to increased DDN assimilation by dinoflagellates but to no change in host tissue (Pogoreutz et al. 2017a), while Rådecker et al. (2021) observed net release of N from the holobiont under heat stress, even preceding bleaching, which was shown to coincide with transcripts pertaining to the catabolism of amino acids in the coral host transcriptome. In this study, the fluxes of DIN and DIP changed with the nutrient concentrations and shifted from net uptake to release in experimental group IV, suggesting that the symbiotic relationships of corals from Weizhou Island were affected by nutrient enrichment despite the absence of coral bleaching.

#### 4.2. Effects of skewed N:P ratios on physiology of coral holobionts

In DIP-limited environments, DOP could support the growth of dinoflagellates (Wiedenmann et al. 2013). Thus, the largest DOP influx was observed in group I with the highest N:P ratio, indicating an



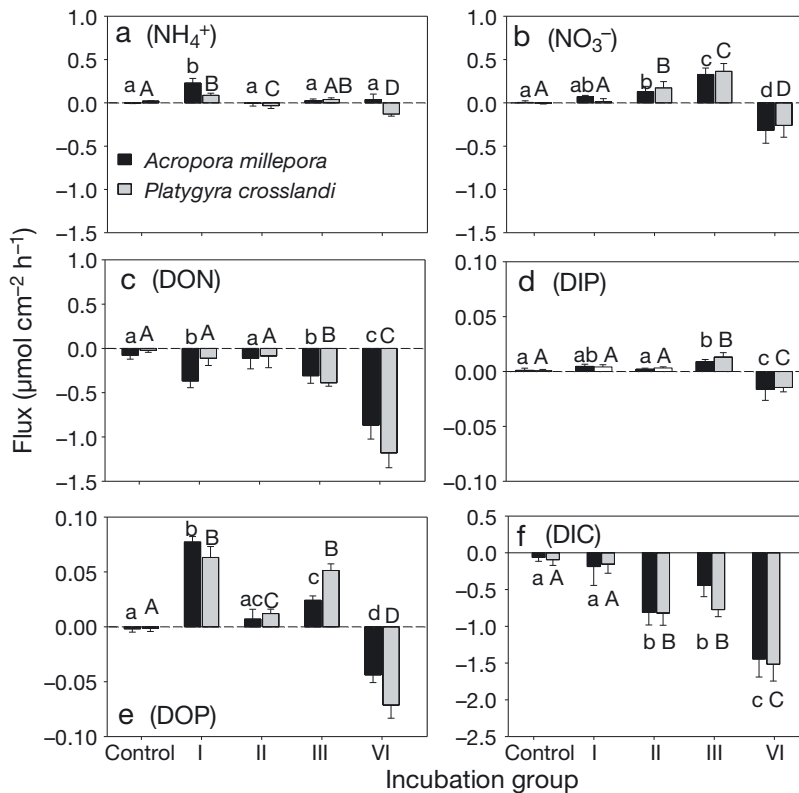


Fig. 4. Fluxes of (a)  $\text{NH}_4^+$ , (b)  $\text{NO}_3^-$ , (c) dissolved organic nitrogen (DON), (d) dissolved inorganic phosphorus (DIP), (e) dissolved organic phosphorus (DOP), and (f) dissolved inorganic carbon (DIC) between seawater and 2 species of corals incubated in 5 different nutrient conditions (see Table 1). The positive values represent rates of nutrient uptake by the coral from the seawater, and the negative values represent rates of nutrient release from the coral to the seawater. The error bars show SD, and different letters above histograms denote statistical differences among varied nutrient conditions (Tukey tests,  $p < 0.05$ )

adaptive regulation mechanism for nutrient uptake by coral holobionts. However, severe P starvation disturbs the symbiosis, as indicated by malfunctioning algal photosynthesis and even expulsion of dinoflagellates (Rosset et al. 2017). Thus, the highest N:P ratio led to the lowest  $\Phi_{\text{PSII}}$  of symbiotic dinoflagellates being  $< 0.5$  and, subsequently, lower N flux in *Platygyra crosslandi* than in *Acropora millepora* (Fig. 4a–c). However, the high N:P ratio did not seem to affect the calcification and DIC flux of corals at the holobiont level.

In addition, the extremely high N:P ratio in group I resulted in a low DDN assimilation rate, and the majority of DDN was primarily assimilated into the tissue, probably also because the N:P ratio was higher in dinoflagellates than in coral tissue (Blanckaert et al. 2020). This could be explained by the ammonia switch-off effect (i.e. immediate inactivation of  $\text{N}_2$  fixation occurs when a superior N source is

encountered) (Kessler et al. 2001, Tilstra et al. 2017): in other words, corals do not waste precious energy on expensive  $\text{N}_2$  fixation if N is abundant. Conversely, DDN assimilation rate increased with increasing P concentration and decreasing N:P ratios, which is consistent with the finding that DDN assimilation strongly varies with P availability and N:P ratios in seawater (Bednarz et al. 2017, Benavides et al. 2017).

#### 4.3. Comparison of the 2 coral species responding to nutrient enrichment and N:P ratios

Tissue thickness contributes to resilience by increasing energy storage (Putnam et al. 2017). In laboratory incubations, we have measured the algal biomass and tissue content of corals, which were greater for *P. crosslandi* than for *A. millepora*. However, there may be no difference in thickness between these corals at Weizhou Island, where corals experience ongoing sediment and nutrient stress (Liao et al. 2019), because tissue thickness can change along a gradient of sediment stress (Barnes & Lough 1999). In this study, none of the metabolic rates differed significantly between the 2 coral species, with the exception of  $\text{NH}_4^+$  flux and DDN assimilation rates, but the rates were measured at the holobiont level (i.e. the oxygen release and the nutrient uptake by symbiotic algae are all folded into the results, thus affecting calcification calculations).

More depleted  $\delta^{13}\text{C}$  in tissue of *A. millepora* than of *P. crosslandi* suggests that *A. millepora* was more heterotrophic than *P. crosslandi* (Lesser et al. 2007, Ferrier-Pagès et al. 2011). Conversely, the  $\delta^{15}\text{N}$  was more enriched in *A. millepora* than in *P. crosslandi*, indicating their variation in nutrient sources with different  $\delta^{15}\text{N}$  (Heikoop et al. 2000).  $\text{N}_2$  fixation was suggested to compensate for the low heterotrophic N uptake in autotrophic corals (Pogoreutz et al. 2017b); thus, DDN assimilation rate by tissue was higher for *P. crosslandi* than for *A. millepora*, leading to more depletion of  $\delta^{15}\text{N}$  in *P. crosslandi* than in *A. millepora*. In particular, *P. crosslandi* tends to be vulnerable to high N:P

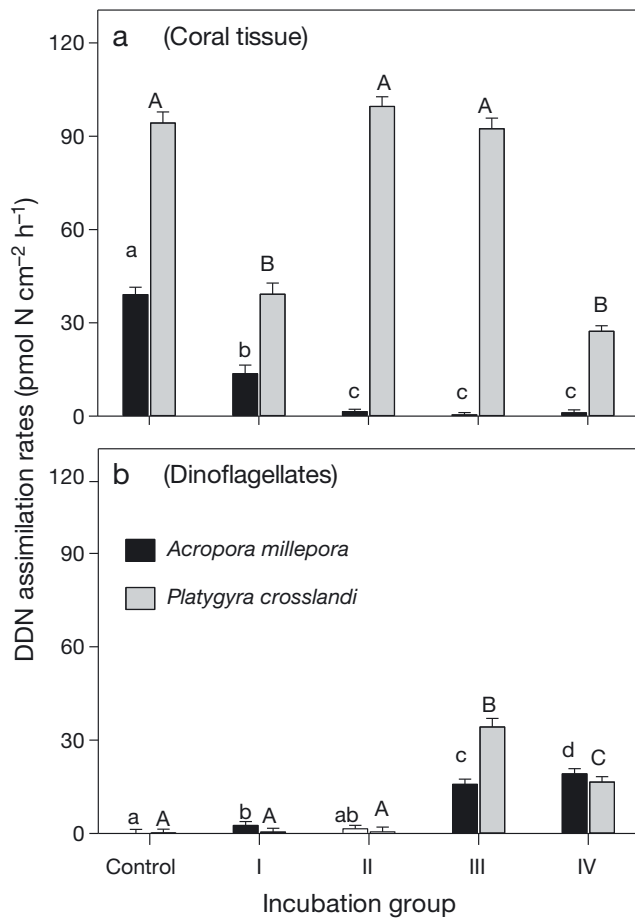


Fig. 5. Diazotroph-derived nitrogen (DDN) assimilation by (a) coral tissue and (b) dinoflagellates of the corals *Acropora millepora* and *Platygyra crosslandi* incubated in 5 different nutrient conditions (see Table 1). The rates are normalized to the coral surface area. The error bars show SD, and different letters above histograms denote statistical differences among varied nutrient conditions (Tukey tests,  $p < 0.05$ )

ratios, resulting in lower  $\Phi_{PSII}$  and  $\text{NH}_4^+$  uptake rate of *P. crosslandi* than of *A. millepora*.

Altogether, we found species-specific as well as dose-dependent responses of Weizhou Island corals to elevated nutrient concentrations and increased ratios. The episodic moderate-level nutrient enrichment will not lead to coral bleaching, but bleaching may be the eventual outcome of the disturbance of nutrient cycling between corals and their symbiotic algae under chronic nutrient enrichment (Rådecker et al. 2021). Although there was no significant difference in the nutrient uptake rates between the 2 coral species at the holobiont level, the differences in  $\delta^{13}\text{C}$ ,  $\delta^{15}\text{N}$ , and DDN showed that *A. millepora* responded more strongly to nutrient enrichment than *P. crosslandi*. Yet it is worth noting that, in the case of an extremely increased N:P ratio, *P. crosslandi* may be

more at risk of thermal bleaching than *A. millepora*, although *P. crosslandi* dominated in the coral assemblages of Weizhou Island. These results shed light on the effect of nutrient enrichment and skewed ratios on corals in relatively high-latitude reefs, but further research is required to assess the potential interaction of climate change and nutrient enrichment on the reefs, which will be beneficial for refining risk management strategies.

**Acknowledgements.** This research was funded by the National Natural Science Foundation of China (Nos. 42030502 and 42090041), the Guangxi Scientific Projects (Nos. AD17129063 and AA17204074), the Guangxi Natural Science Foundation (No. 2019GXNSFAA185001 and 2018GXNSFBA050023), and the Bagui Fellowship from Guangxi Province of China (No. 2014BGXZGX03). We sincerely thank the 3 anonymous reviewers for their valuable comments and suggestions.

#### LITERATURE CITED

- ✦ Barnes DJ, Lough JM (1999) *Porites* growth characteristics in a changed environment: Misima Island, Papua New Guinea. *Coral Reefs* 18:213–218
- ✦ Bednarz VN, Grover R, Maguer JF, Fine M, Ferrier-Pagès C (2017) The assimilation of diazotroph-derived nitrogen by scleractinian corals depends on their metabolic status. *MBio* 8:e02058-16
- ✦ Bednarz VN, van de Water JAJM, Rabouille S, Maguer JF, Grover R, Ferrier-Pagès C (2019) Diazotrophic community and associated dinitrogen fixation within the temperate coral *Oculina patagonica*. *Environ Microbiol* 21: 480–495
- ✦ Bell PRF, Elmetri I, Lapointe BE (2014) Evidence of large-scale chronic eutrophication in the Great Barrier Reef: quantification of chlorophyll *a* thresholds for sustaining coral reef communities. *Ambio* 43:361–376
- ✦ Benavides M, Bednarz VN, Ferrier-Pagès C (2017) Diazotrophs: overlooked key players within the coral symbiosis and tropical reef ecosystems? *Front Mar Sci* 4:10
- ✦ Blanckaert ACA, Reef R, Pandolfi JM, Lovelock CE (2020) Variation in the elemental stoichiometry of the coral–zooxanthellae symbiosis. *Coral Reefs* 39:1071–1079
- ✦ Crandall JB, Teece MA (2012) Urea is a dynamic pool of bioavailable nitrogen in coral reefs. *Coral Reefs* 31: 207–214
- ✦ Ezzat L, Maguer JF, Grover R, Ferrier-Pagès C (2015) New insights into carbon acquisition and exchanges within the coral–dinoflagellate symbiosis under  $\text{NH}_4^+$  and  $\text{NO}_3^-$  supply. *Proc R Soc B* 282:20150610
- ✦ Ezzat L, Fine M, Maguer J, Grover R, Ferrier-Pagès C (2017) Carbon and nitrogen acquisition in shallow and deep holobionts of the scleractinian coral *S. pistillata*. *Front Mar Sci* 4:102
- ✦ Fabricius KE (2005) Effects of terrestrial runoff on the ecology of corals and coral reefs: review and synthesis. *Mar Pollut Bull* 50:125–146
- ✦ Ferrier-Pagès C, Peirano A, Abbate M, Cocito S and others (2011) Summer autotrophy and winter heterotrophy in the temperate symbiotic coral *Cladocora caespitosa*. *Limnol Oceanogr* 56:1429–1438

- Ferrier-Pagès C, Godinot C, D'Angelo C, Wiedenmann J, Grover R (2016) Phosphorus metabolism of reef organisms with algal symbionts. *Ecol Monogr* 86:262–277
- Glud RN, Eyre BD, Patten N (2008) Biogeochemical responses to mass coral spawning at the Great Barrier Reef: effects on respiration and primary production. *Limnol Oceanogr* 53:1014–1024
- Großkopf T, Mohr W, Baustian T, Schunck H and others (2012) Doubling of marine dinitrogen-fixation rates based on direct measurements. *Nature* 488:361–364
- Grover R, Maguer JF, Reynaud-Vaganay S, Ferrier-Pagès C (2002) Uptake of ammonium by the scleractinian coral *Stylophora pistillata*: effect of feeding, light, and ammonium concentrations. *Limnol Oceanogr* 47:782–790
- Heikoop JM, Dunn JJ, Risk MJ, Tomascik T, Schwarcz HP, Sandeman IM, Sammarco PW (2000)  $\delta^{15}\text{N}$  and  $\delta^{13}\text{C}$  of coral tissue show significant inter-reef variation. *Coral Reefs* 19:189–193
- Hillyer KE, Dias D, Lutz A, Roessner U, Davy SK (2018)  $^{13}\text{C}$  metabolomics reveals widespread change in carbon fate during coral bleaching. *Metabolomics* 14:12
- Kessler PS, Daniel C, Leigh JA (2001) Ammonia switch-off of nitrogen fixation in the methanogenic archaeon *Methanococcus maripaludis*: mechanistic features and requirement for the novel *glnB* homologues, *nifI*<sub>1</sub> and *nifI*<sub>2</sub>. *J Bacteriol* 183:882–889
- Koop K, Booth D, Broadbent A, Brodie J and others (2001) ENCORE: The effect of nutrient enrichment on coral reefs. Synthesis of results and conclusions. *Mar Pollut Bull* 42:91–120
- Lam EKY, Chui APY, Kwok CK, Ip AHP and others (2015) High levels of inorganic nutrients affect fertilization kinetics, early development and settlement of the scleractinian coral *Platygyra acuta*. *Coral Reefs* 34:837–848
- Lantz CA, Carpenter RC, Edmunds PJ (2017) Calcium carbonate ( $\text{CaCO}_3$ ) sediment dissolution under elevated concentrations of carbon dioxide ( $\text{CO}_2$ ) and nitrate ( $\text{NO}_3^-$ ). *J Exp Mar Biol Ecol* 495:48–56
- Lesser MP, Falcón LI, Rodríguez-Román A, Enríquez S, Hoegh-Guldberg O, Iglesias-Prieto R (2007) Nitrogen fixation by symbiotic cyanobacteria provides a source of nitrogen for the scleractinian coral *Montastraea cavernosa*. *Mar Ecol Prog Ser* 346:143–152
- Lewis E, Wallace D (1998) Program developed for  $\text{CO}_2$  system calculations. Carbon Dioxide Information Analysis Center, Oak Ridge National Laboratory, Oak Ridge, TN
- Liao Z, Yu K, Wang Y, Huang X, Xu L (2019) Coral–algal interactions at Weizhou Island in the northern South China Sea: variations by taxa and the exacerbating impact of sediments trapped in turf algae. *PeerJ* 7: e6590
- Marsh JA Jr (1970) Primary productivity of reef-building calcareous red algae. *Ecology* 51:255–263
- McMahon A, Santos IR, Cyronak T, Eyre BD (2013) Hysteresis between coral reef calcification and the seawater aragonite saturation state. *Geophys Res Lett* 40: 4675–4679
- Meyer FW, Vogel N, Diele K, Kunzmann A, Uthicke S, Wild C (2016) Effects of high dissolved inorganic and organic carbon availability on the physiology of the hard coral *Acropora millepora* from the Great Barrier Reef. *PLOS ONE* 11:e0149598
- Mohr W, Grosskopf T, Wallace DWR, LaRoche J (2010) Methodological underestimation of oceanic nitrogen fixation rates. *PLOS ONE* 5:e12583
- Morris LA, Voolstra CR, Quigley KM, Bourne DG, Bay LK (2019) Nutrient availability and metabolism affect the stability of coral–Symbiodiniaceae symbioses. *Trends Microbiol* 27:678–689
- Ning Z, Yu K, Wang Y, Huang X, Han M, Zhang J (2019) Carbon and nutrient dynamics of permeable carbonate and silicate sands adjacent to coral reefs around Weizhou Island in the northern South China Sea. *Estuar Coast Shelf Sci* 225:106229
- Ning Z, Fang C, Yu K, Yang B and others (2020) Influences of phosphorus concentration and porewater advection on phosphorus dynamics in carbonate sands around the Weizhou Island, northern South China Sea. *Mar Pollut Bull* 160:111668
- Pogoreutz C, Rådecker N, Cárdenas A, Gärdes A, Voolstra CR, Wild C (2017a) Sugar enrichment provides evidence for a role of nitrogen fixation in coral bleaching. *Glob Change Biol* 23:3838–3848
- Pogoreutz C, Radecker N, Cardenas A, Gardes A, Wild C, Voolstra CR (2017b) Nitrogen fixation aligns with *nifH* abundance and expression in two coral trophic functional groups. *Front Microbiol* 8:1187
- Putnam HM, Barott KL, Ainsworth TD, Gates RD (2017) The vulnerability and resilience of reef-building corals. *Curr Biol* 27:R528–R540
- Rådecker N, Pogoreutz C, Voolstra CR, Wiedenmann J, Wild C (2015) Nitrogen cycling in corals: the key to understanding holobiont functioning? *Trends Microbiol* 23: 490–497
- Rådecker N, Pogoreutz C, Gegner HM, Cardenas A and others (2021) Heat stress destabilizes symbiotic nutrient cycling in corals. *Proc Natl Acad Sci USA* 118: e2022653118
- Rao AMF, McCarthy MJ, Gardner WS, Jahnke RA (2007) Respiration and denitrification in permeable continental shelf deposits on the South Atlantic Bight: rates of carbon and nitrogen cycling from sediment column experiments. *Cont Shelf Res* 27:1801–1819
- Reich HG, Rodríguez IB, LaJeunesse TC, Ho TY (2020) Endosymbiotic dinoflagellates pump iron: differences in iron and other trace metal needs among the Symbiodiniaceae. *Coral Reefs* 39:915–927
- Risk MJ, Sammarco PW, Schwarcz HP (1994) Cross-continental shelf trends in  $\delta^{13}\text{C}$  in coral on the Great Barrier Reef. *Mar Ecol Prog Ser* 106:121–130
- Rohwer F, Seguritan V, Azam F, Knowlton N (2002) Diversity and distribution of coral-associated bacteria. *Mar Ecol Prog Ser* 243:1–10
- Rosset S, Wiedenmann J, Reed AJ, D'Angelo C (2017) Phosphate deficiency promotes coral bleaching and is reflected by the ultrastructure of symbiotic dinoflagellates. *Mar Pollut Bull* 118:180–187
- Shantz AA, Burkepille DE (2014) Context-dependent effects of nutrient loading on the coral–algal mutualism. *Ecology* 95:1995–2005
- Tanaka Y, Miyajima T, Watanabe A, Nadaoka K, Yamamoto T, Ogawa H (2011) Distribution of dissolved organic carbon and nitrogen in a coral reef. *Coral Reefs* 30:533–541
- Tanaka Y, Grottoli AG, Matsui Y, Suzuki A, Sakai K (2017) Effects of nitrate and phosphate availability on the tissues and carbonate skeleton of scleractinian corals. *Mar Ecol Prog Ser* 570:101–112
- Tilstra A, Bednarz VN, Cardini U, van Hoytema N, Al-Rshaidat MMD, Wild C (2017) Seasonality affects dinitrogen

- fixation associated with two common macroalgae from a coral reef in the northern Red Sea. *Mar Ecol Prog Ser* 575:69–80
- ✦ Wiedenmann J, D'Angelo C, Smith EG, Hunt AN, Legiret FE, Postle AD, Achterberg EP (2013) Nutrient enrichment can increase the susceptibility of reef corals to bleaching. *Nat Clim Change* 3:160–164
- ✦ Xu L, Yu K, Li S, Liu G and others (2017) Interseasonal and interspecies diversities of *Symbiodinium* density and effective photochemical efficiency in five dominant reef coral species from Luhuitou fringing reef, northern South China Sea. *Coral Reefs* 36:477–487
- ✦ Xu S, Zhang Z, Yu K, Huang X, Chen H, Qin Z, Liang R (2021) Spatial variations in the trophic status of *Favia palauensis* corals in the South China Sea: insights into their different adaptabilities under contrasting environmental conditions. *Sci China Earth Sci* 64:839–852
- ✦ Yu K (2012) Coral reefs in the South China Sea: their response to and records on past environmental changes. *Sci China Earth Sci* 55:1217–1229
- ✦ Yu W, Wang W, Yu K, Wang Y and others (2019) Rapid decline of a relatively high latitude coral assemblage at Weizhou Island, northern South China Sea. *Biodivers Conserv* 28:3925–3949

*Editorial responsibility: Mirta Teichberg,  
Woods Hole, Massachusetts, USA  
Reviewed by: 3 anonymous referees*

*Submitted: February 5, 2021  
Accepted: October 13, 2021  
Proofs received from author(s): December 11, 2021*